Hindawi
Wireless Communications and Mobile Computing
Volume 2021, Article ID 2835638, 8 pages
https://doi.org/10.1155/2021/2835638

Research Article

Reconfigurable Reflectarray Antenna: A Comparison between Design Using PIN Diodes and Liquid Crystals

Muhammad Inam Abbasi[1], **Muhammad Yusof Ismail**[2], **Muhammad Ramlee Kamarudin**[2] and **Qammer H. Abbasi**[3]

[1]*Centre for Telecommunication Research & Innovation (CETRI), Faculty of Electrical and Electronic Engineering Technology (FTKEE), Universiti Teknikal Malaysia Melaka (UTeM), Melaka 76100, Malaysia*
[2]*Faculty of Electrical and Electronic Engineering (FKEE), Universiti Tun Hussein Onn Malaysia (UTHM), 86400 Batu Pahat, Johor, Malaysia*
[3]*James Watt School of Engineering, College of Science and Engineering, University of Glasgow, Glasgow, UK*

Correspondence should be addressed to Muhammad Inam Abbasi; muhammad_inamabbasi@yahoo.com

Received 27 July 2021; Revised 24 September 2021; Accepted 15 October 2021; Published 29 October 2021

Academic Editor: Farman Ullah

This work presents the design and analysis of active reflectarray antennas with slot embedded patch element configurations within an *X*-band frequency range. Two active reflectarray design technologies have been proposed by digital frequency switching using PIN diodes and analogue frequency tuning using liquid crystal-based substrates. A waveguide simulator has been used to perform scattering parameter measurements in order to practically compare the performance of reflectarray designed based on the two active design technologies. PIN diode-based active reflectarray unit cell design is shown to offer a frequency tunability of 0.36 GHz with a dynamic phase range of 226°. On the other hand, liquid crystal-based design provided slightly lower frequency tunability of 0.20 GHz with a dynamic phase range of 124°. Moreover, the higher reflection loss and slow frequency tuning are demonstrated to be the disadvantages of liquid crystal-based designs as compared to PIN diode-based active reflectarray designs.

1. Introduction

A reflectarray, as suggested by the name, is a flat reflecting array of resonant patch elements that can be used for a number of applications where high gain antennas are required. Some of the main characteristics of a reflectarray antenna are its lower cost, lower mass, and smaller stowage volume, which is generally demanded in the spacecraft antennas in order to reduce payload weight and required shroud space to minimize overall launch cost. Conventionally, high-gain applications have counted on parabolic reflectors and phased arrays [1]. Nevertheless, due to the curvature of their surface, parabolic reflectors are challenging to be manufactured in many cases at higher microwave frequencies [2]. The shape of the parabolic reflector also causes an increase in the weight and size of the antenna. Moreover, it has also been established in [3] that wide-angle electronic beam scanning cannot be achieved using a parabolic reflector. On the other hand, high-gain phased array antennas offer the opportunity to electronically scan the main beam along wide-angle positions provided that they are equipped with controllable phase shifters. However, the main shortcoming of phased array antennas is their large hardware footprint, as each element of an array or subarray needs to be connected to a dedicated transceiver module. These modules are usually high profile, thus making phased array antennas a costly solution for high-gain applications.

Direct Broadcast Satellites (DBS) and Multibeam Antennas (MBA) are also considered potential applications of reflectarrays apart from recent investigations on their applicability in 5G communication systems [4–7]. Reflectarrays can also be used as amplifying arrays by adding an amplifier in each of the unit cells [8]. Despite many potentials, the main shortcomings of a reflectarray antenna are its limited

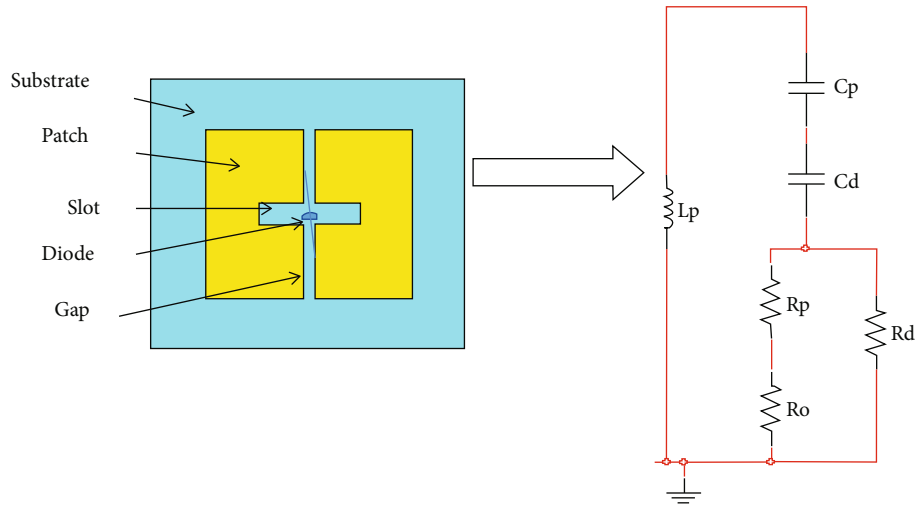

Figure 1: PIN diode-based unit cell with equivalent circuit representation.

bandwidth and high loss performance as compared to the parabolic reflector antennas [9–11]. Researchers have proposed a number of configurations in the past few years for the bandwidth and loss performance improvement of reflectarrays [12–16]. However, considerable efforts are still required to improve the bandwidth performance of reflectarrays. In order to steer the main beam of an active reflectarray, the reflected phase from each of the resonant elements can be controlled. Therefore, the reflected beam can be directed in the desired direction, which makes a reflectarray capable of achieving a wide-angle electronic beam scanning. Such a beamforming approach can have many advantages over traditional tunable antenna array architectures, including a significant reduction in hardware required per element and increased efficiency [17]. There has been considerable research in beam steering of reflectarray antennas such as the use of nonlinear dielectric materials [18–20] and the integration of Radio Frequency Micro-Electro-Mechanical Systems (RF MEMS) as switches [21, 22], using aperture-coupled elements where the tuning circuit can be located on the nonresonating surface of the element in order to control the contributed phase from each element [23] and using mechanical movement of the antenna [24].

In this work, slot embedded patch element configurations have been proposed for active reflectarray designs. PIN diodes have been proposed to be incorporated directly on the resonant elements for frequency switching in reflectarrays, while liquid crystals have been proposed in separate designs to be used as a substrate for tunable reflectarray design. The 3D EM computer simulation software results of CST MWS and Ansoft HFSS have been verified using waveguide scattering parameter measurements. Detailed comparisons between different performance parameters of the two design technologies are discussed in this work. Commercially available computer models of CST Microwave Studio and Ansoft HFSS were used to design unit cell patch elements with proper boundary conditions in order to analyze the scattering parameters of an infinite reflectarray. Initially, a reflectarray with a rectangular patch element was designed to resonate at 10 GHz using Rogers RT/Duroid 5880 ($\varepsilon r = 2.2$ and $\tan\delta = 0.0010$) as a substrate with a thickness of 0.3818 mm. Then, rectangular slot configurations are introduced in the patch element, and the effect on the performance of the reflectarray was observed. Reflectarray unit cells consisting of two patch elements were used for the waveguide scattering parameter measurements [25].

2. Frequency Switchable Reflectarray Design Using PIN Diodes

In this work, apart from the rectangular slot, a vertical gap was introduced in the resonant slot embedded patch element for the practical implementation of PIN diodes. This gap provides an option to connect the diode in a way that it can have different potentials at the two connecting ends. Moreover, the vertical gap does not affect the resonance performance of the unit cell as the maximum surface currents were observed to be along the width of the patch and slots.

PIN diodes were integrated in the gap introduced on the slot embedded patch element. Scattering parameter measurements were carried out for a unit cell that comprised two patch elements with dimensions of $L_p \times W_p = 9.4\,\text{mm} \times 10\,\text{mm}$ each, which were printed on a substrate of $L_s \times W_s = 15\,\text{mm} \times 30\,\text{mm}$ (L_p and W_p are the length and width of the patch element, respectively, while L_s and W_s are the length and width of the substrate, respectively). The slot length was kept at 0.6 mm, while the width was 0.5 W_p. The vertical gap was introduced with a 0.6 mm width in order to fit the PIN diode. Figure 1 shows the unit cell of the PIN diode-based planar reflector with its equivalent circuit representation. Equivalent circuits can also be used for the characterization of the planar reflector unit cells based on the lumped components. In this design, L_p, C_p, and R_p represent inductance, capacitance, and resistance of a passive planar reflector unit cell, respectively, while C_d, R_o, and R_d are used to represent the on and off states of the PIN diodes. For the electronic switching of PIN diode-based design, a GaAS MA4GP907 PIN diode manufactured by

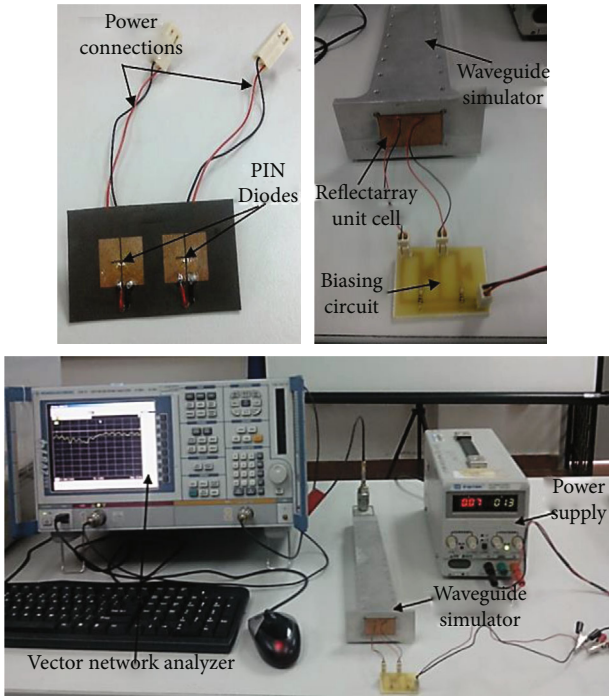

Figure 2: Fabricated unit cell, biasing circuit, and complete measurement setup.

MACOM was used. This PIN diode has a series capacitance of 0.025 pF and low series resistance of 4.2 Ω.

Figure 2 shows the fabricated unit cell, the biasing circuit connected with the unit cell, and the complete setup for scattering parameter measurements. As shown in Figure 2, the PIN diodes were soldered on the surface of the patch element and were powered by a power supply using a biasing circuit. A high-accuracy SMT fabrication facility was used to solder the PIN diodes on the resonant patch structure as accurately as possible. 1.33 V were supplied and a 100 Ω resistor was used to forward bias the diodes while no negative voltage (0 V) was required to reverse bias the diodes. RF choke was implemented using quarter-wavelength segments and radial stub on the biasing circuit. DC block capacitors were not required in this case because there is no physical connection between the RF source (network analyzer) and DC source (power supply).

Reflection loss and reflection phase were measured within an X-band frequency range, and a close agreement between measured and simulated results was observed. Figure 3 shows a comparison between measured and simulated reflection loss curves for fabricated samples. It can be observed from Figure 3 that in the off state of the PIN diode, the measured resonant frequency is close to the simulated resonant frequency. The fabricated unit cell resonated at 9.40 GHz with a reflection loss of 2.60 dB while the simulations for the off state of the PIN diode provided a resonant frequency of 9.38 GHz with 1.61 dB reflection loss. When the PIN diodes were switched on, a clear change in frequency was observed for the fabricated samples. In the on state, the measured resonant frequency was observed to be 9.04 GHz with a reflection loss of 3.91 dB. In comparison,

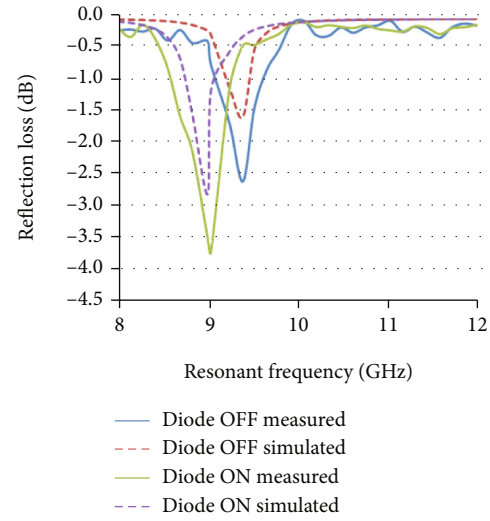

Figure 3: Comparison between simulated and measured reflection loss curves of PIN diode-based active reflectarrays.

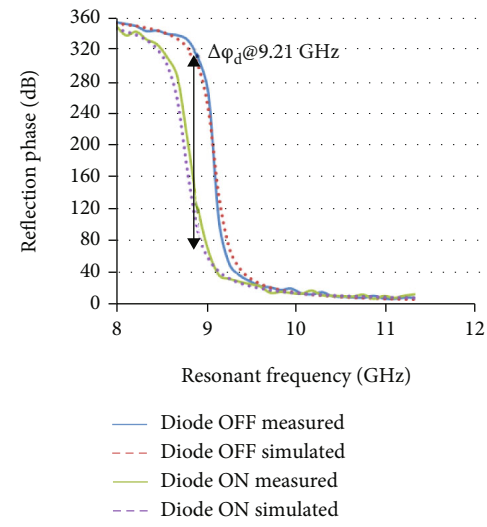

Figure 4: Comparison between simulated and measured reflection phase curves of PIN diode-based active reflectarrays.

the simulation results for the on state of the PIN diode exhibited a reflection loss of 2.88 dB at a resonant frequency of 8.99 GHz.

The highest discrepancy between measured and simulated reflection loss was observed to be 0.99 dB and 1.03 dB in off and on states of PIN diodes, respectively. Moreover, extra noise or ripples with a maximum level of 0.25 dB were observed. The reason for this discrepancy is due to fabrication quality, including the soldering of PIN diodes and the difference between actual material properties and the properties given in the datasheet. Furthermore, the diode was intentionally placed tilted in order to optimize the reflection loss and reflection phase results in simulations. The optimization was carried out keeping in mind the maximum current distribution on the surface of the patch. However, in measurements, it was not possible to place the diode at the

Table 1: Comparison between simulated and measured frequency tunability and dynamic phase range.

Results		Frequency tunability Fr (GHz)	Dynamic phase range $\Delta\varphi d$ (°)
Simulated	CST MWS	0.41	231
	Ansoft HFSS	0.39	228
Measured results		0.36	226

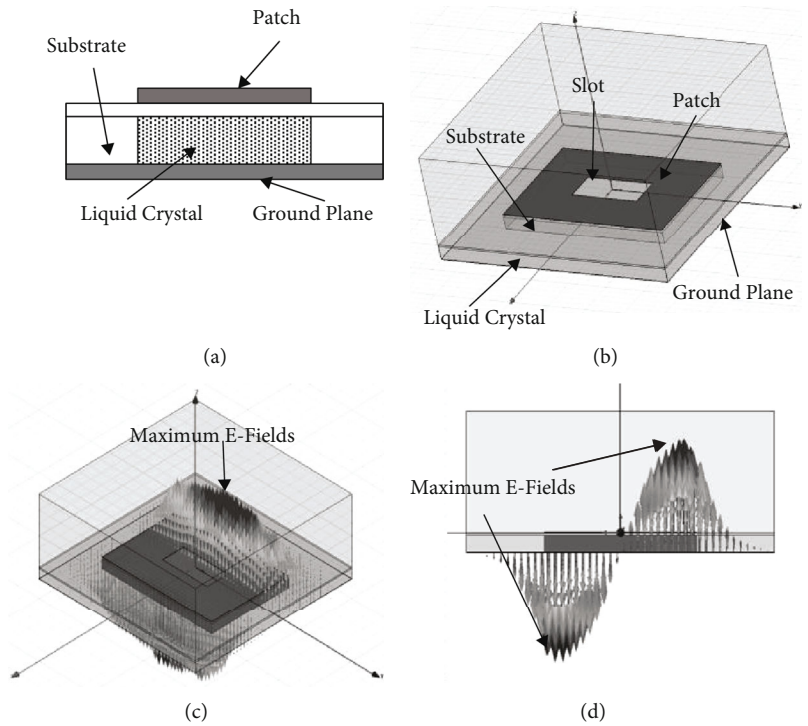

Figure 5: Active reflectarray unit cell design: (a) perspective view of a rectangular slot embedded patch element unit cell; (b) illustrative side view; (c) E-fields from a perspective view; (d) E-fields from a side view.

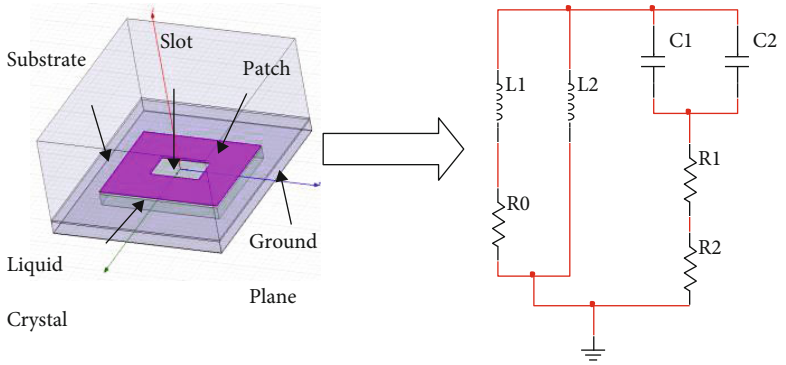

Figure 6: LC-based unit cell with equivalent circuit representation.

exact location as in simulations, because of the diode dimensions and fabrication complexity. The positioning of the diode can also be a possible reason to add up to the discrepancy in the results as shown in Figure 3. The discrepancy can be minimized with the more careful fabrication of unit cells and a thorough investigation of the actual material properties of the substrate used after going through the fabrication process. Figure 4 shows a comparison between the measured and simulated reflection phases. A close agreement between the measured and simulated phases can be observed from

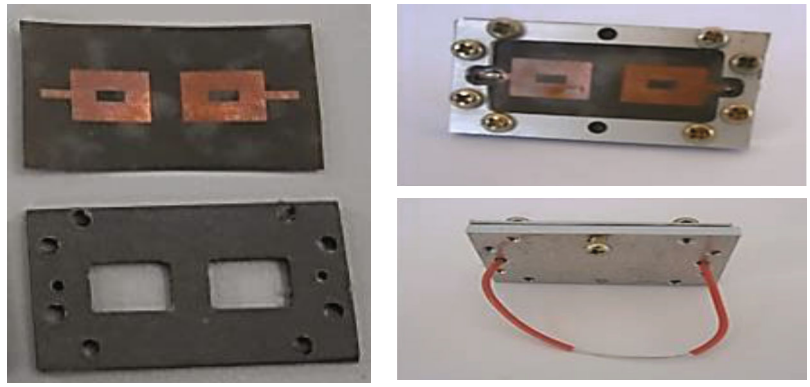

(a) (b)

Figure 7: Fabricated samples: (a) unit cell patch element and LC cavity; (b) rectangular slot embedded path and back side of complete unit cell assembly in an encapsulator.

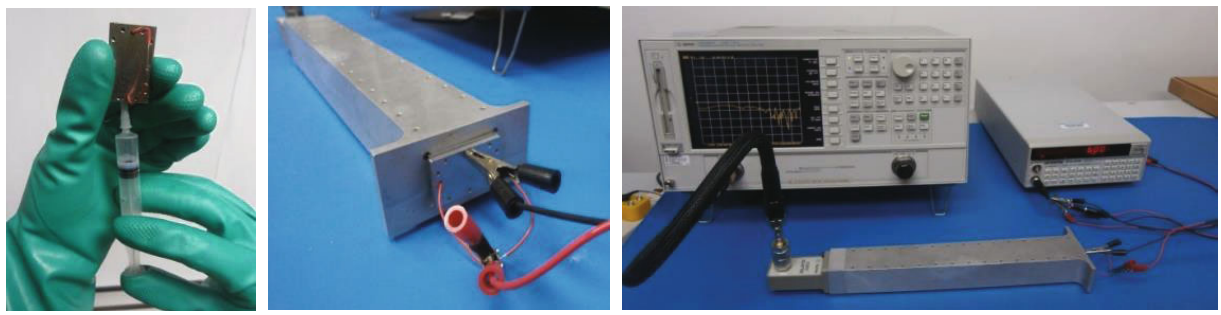

Figure 8: LC filling in a cavity, a unit cell inserted in a waveguide simulator, and complete measurement setup for scattering parameter measurements.

Figure 4, except for the ripples found towards the edges of the measured curves. These ripples can be linked to the same sources, which caused a discrepancy in the reflection loss curves. Table 1 provides a comparison between simulated and measured results of the frequency tunability and dynamic phase range. The dynamic phase range was calculated at the central frequency of two resonant curves in off and on states of PIN diodes as shown in Figure 4. It can be observed from Table 1 that a maximum frequency tunability of 0.36 GHz and a dynamic phase range of 226° were demonstrated by PIN diode base unit cell measurements. The results are in close agreement with the results obtained by 3D EM simulators of CST MWS and Ansoft HFSS, which practically validates the proposed design.

3. Reconfigurable Reflectarray Design Using Liquid Crystal Substrates

The change in the molecular orientation of liquid crystals (LC) can be done by applying a bias voltage [26, 27]. This change in molecular orientation gives rise to the dielectric anisotropy ($\Delta\varepsilon$) of LC, which makes them suitable to be used as a tunable dielectric substrate in reflectarrays. $\Delta\varepsilon$ can be explained as

$$\Delta\varepsilon = \varepsilon_{\parallel} - \varepsilon_{\perp}, \tag{1}$$

where $\varepsilon\perp$ and $\varepsilon\parallel$ are the magnitude of the dielectric constant measured perpendicular and parallel to the applied electric field. The reflection phase and resonant frequency of reflectarrays can be tuned for various values with the help of an external tunable bias voltage [16].

The basic design topology of a unit cell reflectarray with periodic boundary conditions has been used in Ansoft HFSS to represent a single patch element as an infinite array. The resonant patches, as shown in Figures 5(a) and 5(b), have been fabricated on a thin supporting layer of Rogers RT/Duroid 5880 with a substrate thickness of 0.127 mm. K-15 nematic LC has been deposited within a cavity made in the dielectric substrate of Rogers RT/Duroid 5880 with a substrate thickness of 0.787 mm backed by a ground plane. The dimensions of the resonant patch element are kept 8.4 mm × 11.8 mm ($L \times W$) for resonance within an X-band frequency range. It can be observed from Figures 5(c) and 5(d) that the E-fields are sinusoidally distributed with maxima at the corners of the resonant patch element. Therefore, the surface currents will be maximum in the centre of the patch element along the direction of field excitation (x-axis).

Figure 6 shows the equivalent circuit representation of an LC-based unit cell planar reflector design. Apart from the basic RLC circuit, extra inductance, capacitance, and resistance have to be considered because of the introduction of liquid crystal under the patch element within the solid substrate cavity.

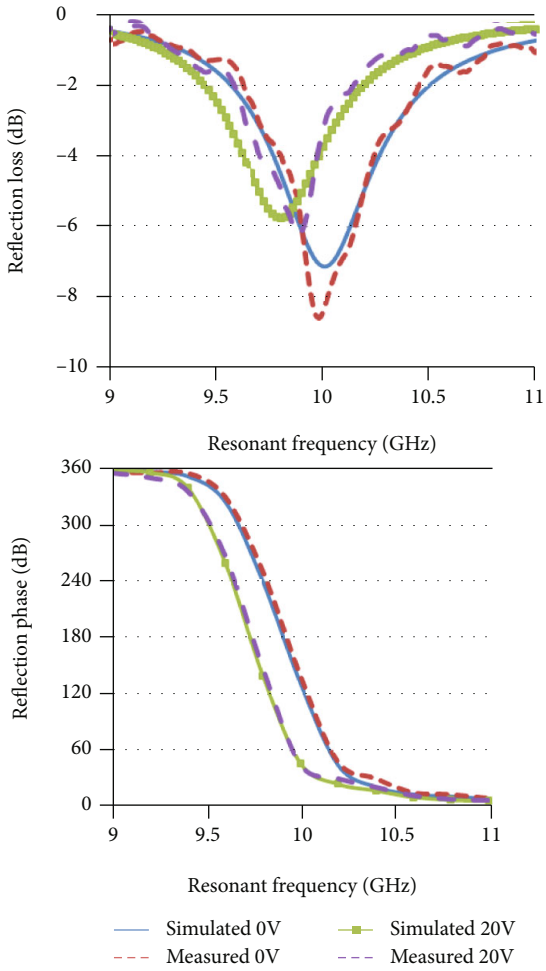

Figure 9: Comparison of measured and simulated results for a rectangular slot embedded patch element unit cell reflectarray.

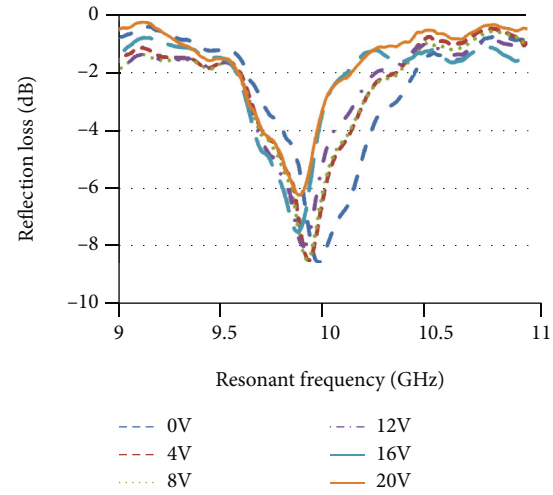

Figure 10: Measured reflection loss curves for different voltage levels applied to LC of unit cell designs.

Table 2: Measured performance comparison between the PIN diodes and liquid crystal-based planar reflectors at an X-band frequency range.

Technology	Frequency tunability (GHz)	Dynamic phase range ($\Delta\varphi d$) (°)	Static phase range ($\Delta\varphi s$) (°)	Tunable loss factor (dB)
PIN diodes	0.36	226	270	1.43
Liquid crystal	0.20	124	260	1.91

In order to design a frequency tunable reflectarray unit cell, the properties of K-15 nematic LC have been exploited. For this type of LC, a voltage variation from 0 V to 20 V can be applied to change the orientation of K-15 nematic LC molecules from perpendicular ($\varepsilon r = 2.7$ and $\tan\delta = 0.04$) to parallel ($\varepsilon r = 2.9$ and $\tan\delta = 0.03$). Different rectangular slot embedded unit cell patch elements have been fabricated for X-band frequency range operations, as shown in Figure 7(a). Encapsulations made of aluminium shown in Figure 7(b) have been used to keep intact different parts of unit cells, and a connecting wire has been used to electrically short the two patches in order to apply the desired voltage. Figure 8 shows the measurement procedure and LC filling inside the cavity constructed under the resonant patch element. The complete assembly of unit cell patch elements filled with LC has been inserted in the aperture of the waveguide, and scattering parameter measurements have been carried out using a waveguide simulator with a vector network analyzer while the voltage from 0 V to 20 V has been supplied by a function generator to the resonant patch elements.

The scattering parameter measurements of the LC-based rectangular slot embedded patch element unit cells have been carried out, and a comparison between simulated and measured results has been presented in Figure 9. The simulated and measured results provided a close agreement with a variation in measured resonant frequency from 10 GHz to 9.88 GHz with an increase in voltage from 0 V to 20 V. Moreover, a dynamic phase range of 103° measured from the reflection phase curve has been demonstrated by the proposed design of a reconfigurable LC-based unit cell.

In order to further investigate the proposed design, different voltage levels have been applied to K-15 nematic LC and the effect on reflection loss and resonant frequency has been observed, as shown in Figure 10. It can be observed that each increment in voltage level contributes to a small frequency tunability, which reaches to 180 MHz at 20 V level. It can also be observed from Figure 10 that the reflection loss also decreases from 8.5 dB at 10 GHz to 6.2 dB at 9.88 GHz with an increase in voltage from 0 to 20 V. The decrease in reflection loss is because of a decrease in loss tangent value of K-15 nematic LC material from 0.04 to 0.03 with an increase in voltage from 0 to 20 V.

4. Comparative Summary

Active planar reflectors using PIN diodes and liquid crystals provided interesting results for the design for switchable planar reflectors for beam shaping realization in an X-band

Table 3: General comparison between the PIN diodes and liquid crystal base planar reflector design ("+," "0," and "-" symbols refer to good, neutral, and poor, respectively).

Technology	Control	Complexity (cost)	Loss	Switching time
PIN diodes	Digital	0	+	+
Liquid crystal	Analogue	0	-	-

frequency range. The measured results for PIN diode embedded configurations provided a maximum frequency tunability of 0.36 GHz with a dynamic phase range of 226° as compared to those for liquid crystal-based cells, which demonstrated a maximum frequency tunability of 0.20 GHz with 124° of the dynamic phase range. Moreover, the static phase range, which is a measure of phase errors in a planar reflector design, provided a higher range of 270° in the case of PIN diode-based design as compared to the static phase range of 260° demonstrated by liquid crystal-based design. Although a range of frequency tunability options is achievable for liquid crystal-based cells by applying different voltage levels, huge time consumption between 102 S and 840 S is one of the main disadvantages of this design. On the other hand, PIN diode embedded unit cells can provide a fast frequency switching depending on the switching time of the PIN diodes. The diode used in this work (MACOM MA4GP907) has a switching time of 2-3 nS, which provides PIN diode embedded design and edge over liquid crystal-based planar reflector design.

Furthermore, the PIN diode embedded planar reflector unit cell exhibited a maximum measured reflection loss of 3.91 dB, which is much lesser as compared to the 8.56 dB of reflection loss observed for liquid crystal-based unit cell design. The tunable loss factor, which is measured as the difference of reflection loss between the two extreme tunable frequencies, is also higher (1.91 dB) in the case of liquid crystal-based design as compared to PIN diode-based design (1.43 dB). A higher tunable loss factor can be attributed to the properties of the liquid crystals used in the design. Table 2 provides the measured performance comparison for the planar reflector design using the two technologies.

Additionally, as far as the complexity of design is concerned, a uniform deposition layer is required in the case of LC-based design in order to achieve full anisotropy of LC molecules. Moreover, keeping the liquid crystal fully filled inside the cavity is a challenging task and requires a perfect design of the encapsulator. On the other hand, because of the tiny size of the PIN diodes, it was difficult to handle and solder the diodes on the resonant patch elements. However, professional skills and equipment can help to resolve these problems. A general summary of the outcomes of the two design techniques is provided in Table 3.

5. Conclusions

Slot embedded patch element configurations have been identified as a potential configuration for the improved design of passive and reconfigurable reflectarray antennas. The slot embedded patch elements also provide an extra parameter, which is the dimensions of the slot for the control of the resonant frequency and reflection phase of the reflectarray antenna. PIN diode-based design provides a number of advantages over liquid crystal-based design in terms of frequency tunability, dynamic phase range, static phase range, and tunable loss factor. However, liquid crystal-based design provides an edge over PIN diode-based active reflectarray design because of analogue control, which provides the option of tunability over a range of frequencies. It can be concluded from this investigation that there is a trade-off between the performance parameters and continuous tunability achieved by LC-based design. Further investigations are required to improve the frequency tunability and reflection loss performance of reconfigurable reflectarray antennas by investigating the properties of materials and the applied electronic components.

Data Availability

Data is available on request. The corresponding author can be contacted for any relevant data.

Conflicts of Interest

The authors declare that they have no conflicts of interest.

Acknowledgments

Research funding for this work is fully provided by the Ministry of Higher Education, Malaysia, under Best Project of Fundamental Research Grant Scheme (FRGS, VOT 0983), Prototype Research Grant Scheme (PRGS, VOT 0904), and Research Acculturation Collaborative Effort (RACE, VOT 1119).

References

[1] G. D. G. Berry, R. G. Malech, and W. A. Kennedy, "The reflectarray antenna," *IEEE Transactions on Antennas and Propagation*, vol. 11, no. 6, pp. 645–651, 1963.

[2] J. Huang and J. A. Encinar, *Reflectarray Antennas*, vol. 30, John Wiley & Sons, New York, USA, 2007.

[3] J. A. Encinar, M. Arrebola, M. Dejus, and C. Jouve, "Design of a 1-metre reflectarray for DBS application with 15% bandwidth," in *First European Conference on Antennas and Propagation (EUCAP)*, pp. 1–5, Nice, France, 2006.

[4] M. H. Dahri, M. H. Jamaluddin, M. Inam, and M. R. Kamarudin, "A review of wideband reflectarray antennas for 5G communication systems," *IEEE Access*, vol. 5, pp. 17803–17815, 2017.

[5] M. H. Dahri, M. Inam, M. H. Jamaluddin, and M. R. Kamarudin, "A review of high gain and high efficiency reflectarrays for 5G communications," *IEEE Access*, vol. 6, no. 1, pp. 5973–5985, 2018.

[6] M. H. Dahri, M. H. Jamaluddin, M. Khalily, M. Inam, R. Selvaraju, and M. R. Kamarudin, "Polarization diversity and adaptive beamsteering for 5G reflectarrays: a review," *IEEE Access*, vol. 6, no. 1, pp. 19451–19464, 2018.

[7] M. Inam, M. H. Dahri, M. H. Jamaluddin, N. Seman, M. R. Kamarudin, and N. H. Sulaiman, "Design and characterization of millimeter wave reflectarrays for 5G communication

systems," *International Journal of RF and Microwave Computer Aided Engineering*, no. article e21804, 2019.

[8] M. E. Bialkowski, A. W. Robinson, and H. J. Song, "Design, development and testing of X-band amplifying reflectarrays," *IEEE Transactions on Antennas and Propagation*, vol. 50, no. 8, pp. 1065–1076, 2002.

[9] M. Y. Ismail and M. Inam, "Resonant elements for tunable reflectarray antenna design," *International Journal of Antennas and Propagation*, vol. 2012, 6 pages, 2012.

[10] M. E. Biallowski and J. Encinar, "Reflectarray: potential and challenges," *International Conference on Electromagnetics in Advanced Applications*, pp. 1050–1053, 2007.

[11] D. M. Pozar and S. D. Targonski, "A shaped-beam microstrip patch reflectarray," *IEEE Transactions on Antennas propogation*, vol. 47, no. 7, pp. 1167–1173, 1999.

[12] J. Huang and J. Encinar, *Reflectarray Antennas: Broadband Techniques*, Wiley, Interscience, New York, 2007.

[13] M. Y. Ismail and M. Inam, "Performance improvement of reflectarrays based on embedded slots configurations," *Progress In Electromagnetics Research C*, vol. 14, pp. 67–78, 2010.

[14] M. Fazaelifar, S. Jam, and R. Basiri, "Design and fabrication of a wideband reflectarray antenna in Ku and K bands," *AEU - International Journal of Electronics and Communications*, vol. 95, pp. 304–312, 2018.

[15] G. T. Chen, Y. C. Jiao, and G. Zhao, "A reflectarray for generating wideband circularly polarized orbital angular momentum vortex wave," *IEEE Antennas and Wireless Propagation Letters*, vol. 18, pp. 182–186, 2019.

[16] M. Karimipour and I. Aryanian, "Demonstration of broadband reflectarray using unit cells with spline-shaped geometry," *IEEE Transactions on Antennas and Propagation*, vol. 67, pp. 3831–3838, 2019.

[17] S. V. Hum, M. Okoniewski, and R. J. Davies, "Realizing an electronically tunable reflectarray using varactor diode-tuned elements," *IEEE Microwave and Wireless Components Letters*, vol. 15, pp. 422–424, 2005.

[18] S. Costanzo, F. Venneri, and G. D. Massa, "Liquid crystal-based reconfigurable reflectarray cells for 5G systems," in *2019 23rd International Conference on Applied Electromagnetics and Communications (ICECOM)*, pp. 1–3, Dubrovnik, Croatia, 30 Sept.-2 Oct. 2019.

[19] L. Cai, Z. H. Jiang, and W. Hong, "Evaluation of reconfigurable reflectarray antenna element at 19 GHz based on highly anisotropic liquid crystal material," in *2019 IEEE International Conference on Computational Electromagnetics (ICCEM)*, pp. 1–3, Shanghai, China, March 2019.

[20] M. Y. Ismail, M. Inam, and J. Abdullah, "Design optimization of reconfigurable reflectarray antenna based on phase agility technique," in *Proceedings of the 3rd Conference on Antenna & RCS Measurement (ATMS '10),*, vol. 33, pp. 1–5, Delhi, India, 2010.

[21] O. Bayraktar, O. A. Civi, and T. Akin, "Beam switching reflectarray monolithically integrated with RF MEMS switches," *IEEE Transactions on Antennas and Propagation*, vol. 60, no. 2, pp. 854–862, 2012.

[22] F. Tabarani, T. Chaloun, T. Purtova, M. Kaynak, and H. Schumacher, "0.25μm BiCMOS system-on-chip with four transceivers for Ka-band active reflectarrays," in *2015 SBMO/IEEE MTT-S International Microwave and Optoelectronics Conference (IMOC)*, pp. 1–5, Porto de Galinhas, Brazil, November 2015.

[23] M. Riel and J. J. Laurin, "Design of an electronically beam scanning reflectarray using aperture-coupled elements," *IEEE Transactions on Antennas and Propagation*, vol. 55, no. 5, pp. 1260–1266, 2007.

[24] M. I. Abbasi, M. H. Dahri, M. H. Jamaluddin, N. Seman, M. R. Kamarudin, and N. H. Sulaiman, "Millimeter wave beam steering reflectarray antenna based on mechanical rotation of array," *IEEE Access*, vol. 7, pp. 145685–145691, 2019.

[25] M. Inam and M. Y. Ismail, "Reflection loss and bandwidth performance of X-band infinite reflectarrays: simulations and measurements," *Microwave and Optical Technology Letters*, vol. 53, no. 1, pp. 77–80, 2011.

[26] E. Lueder, *Liquid Crystal Displays: Addressing Schemes and Electro-Optical Effects*, John Wiley and Sons, New York, 2nd edition, 2010.

[27] J. Goodby, P. J. Collings, T. Kato, C. Tschierske, H. Gleeson, and P. Raynes, *Handbook of Liquid Crystals*, John Wiley and Sons, New York, 2nd Edition edition, 2014.